Journal of Materials Science & Technology 141 (2023) 193–198

Contents lists available at ScienceDirect

Journal of Materials Science & Technology

journal homepage: www.elsevier.com/locate/jmst

Research Article

A unified model for ductile-to-brittle transition in body-centered cubic metals

Yu-Heng Zhang, En Ma, Jun Sun, Wei-Zhong Han*

State Key Laboratory for Mechanical Behavior of Materials, Xi'an Jiaotong University, Xi'an 710049, China

ARTICLE INFO

Article history:
Received 29 June 2022
Revised 15 August 2022
Accepted 21 August 2022
Available online 28 October 2022

Keywords:
Metals
Ductile
Brittle
Dislocation
Mobility

ABSTRACT

Ductile-to-brittle transition (DBT) is a well-known phenomenon in body-centered-cubic (BCC) metals, intermetallics and semiconductor materials. A quantitative prediction of the DBT temperature, however, has so far remained intractable. Here, we propose a unified model based on the efficacy of dislocation multiplication as the controlling factor for DBT, with the dislocation source efficiency governed by the relative mobility of screw versus edge dislocations. The model successfully predicts the DBT temperature of iron, molybdenum and tungsten, and also covers the influence of grain size, initial dislocation density, and the multiplicity of dislocation sources. A comparison with experiments indicates that the model captures the key DBT features, providing new insight into the toughness of BCC metals.

1. Introduction

The phenomenon of ductile-to-brittle transition (DBT) is ubiquitous in materials, in particular body-centered cubic (BCC) metals [1–6]. Upon cooling to the DBT temperature (DBTT), BCC metals display an abrupt transition from ductile deformation to cleavage brittle fracture, limiting the temperature window for the application of these materials [4–6]. The brittleness/toughness of a material depends on the ability of dislocations to blunt crack propagation. Dislocation activities at the crack tip has two toughening effects: an effective shielding of the crack from the applied load, and the blunting of the crack tip that tends to concentrate the stress to further open the crack [4–6]. Crack-tip plasticity comprises two distinct processes, nucleation of dislocations at or near the crack tip, and their propagation away from the crack. Consequently, two competing mechanisms based on the difficulty in either dislocation nucleation [5] or dislocation movement [6] are proposed to explain the DBT in BCC metals. Specifically, the DBT properties of BCC metals is closely related to the nucleation and gliding of dislocations, in particular, the ½ < 111 > screw dislocation, which has a dissociated, three-dimensional core structure [7–9]. The low-temperature plasticity of BCC metals is thought to be controlled by the kink-pair mechanism of screw dislocations, which displays a strong temperature-dependent behavior [6–11]. Therefore, there is a debate as to whether the nucleation or glide of screw dislocations controls the DBT. Moreover, the physical mechanism underlying the DBT is still incomplete because the thermally activated processes of dislocation nucleation or migration does not directly lead to a sudden transition of the deformation ability of metals.

Recently, through nanoindentation pop-in tests, the temperature-dependent dislocation nucleation stress and glide speed were quantitatively evaluated in BCC chromium (Cr) [10]. As expected, there is no abrupt transition in both the dislocation nucleation stress and the mobility of screw dislocations, thus the critical feature of DBT cannot be explained. Notably, there is a clear correlation between the DBT and the relatively mobility of screw versus edge dislocations (v_s versus v_e) [10,11]. The relatively mobility of dislocations determines the efficiency of dislocation multiplication, which governs the number of dislocations participating in plasticity, thus controlling the brittleness/toughness of BCC metals. Once a critical $\alpha = v_s/v_e$ is reached, for example, $\alpha = 0.7$ for well-annealed coarse-grained Cr, the DBT occurs. The relative mobility of screw versus edge dislocation controls the dislocation source efficiency, which can qualitatively explain the DBT in BCC metals. Nevertheless, how to quantitatively compute the temperature-dependent dislocation multiplications and their relationship with the DBT still remains a challenge. Furthermore, several experimental investigations demonstrate that the DBTT of a BCC metal is not a fixed value, which can be tuned via pre-deformation or introducing substructures [11–16]. For some cases, the DBTT can be reduced by more than 500 K via severe plastic deformation [13]. Therefore, a unified model covering both the temperature-dependent dislocation multiplication and the effect

* Corresponding author.
E-mail address: wzhanxjtu@mail.xjtu.edu.cn (W.-Z. Han).

https://doi.org/10.1016/j.jmst.2022.08.038
1005-0302/

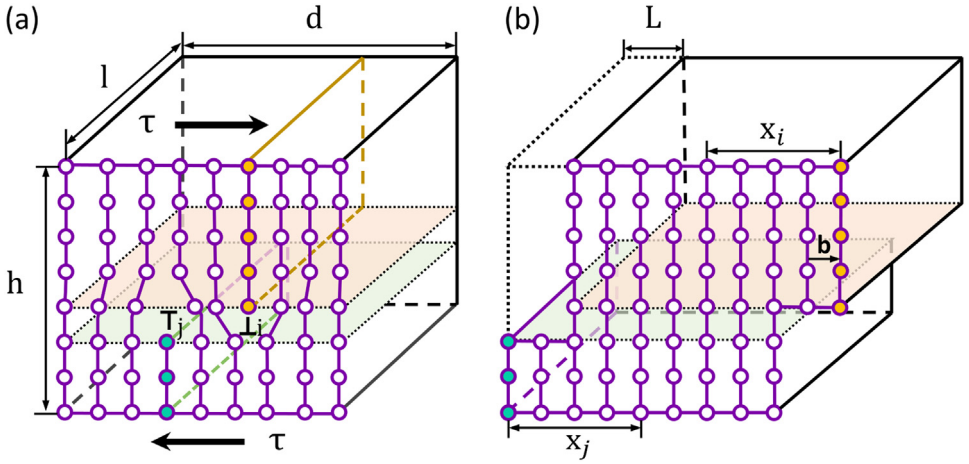

Fig. 1. Sketch of dislocation plasticity. (a) A crystal of volume hld contains edge dislocations gliding with external shear stress, in which colorful surfaces represent the slip planes. (b) Plastic displacement L produces by glide of dislocations, positive ones to the right, negative ones to the left. The x_i and x_j represent corresponding dislocations slip distances.

of microstructural features is needed to better explain the DBT in BCC metals.

In the existing models [17,18], the crack tip plasticity [17] or the dislocation loop expansion [18] mechanism was involved to qualitatively explains the DBT behavior in BCC materials. In this work, however, we develop a theoretical model based on the relative dislocation velocity of screw versus edge dislocations. With the current model, we can quantitatively forecast all the key features of DBT in experiments, including the DBTT, the influence of grain size, initial dislocation density, and the number of microstructural variants that serve as dislocation sources.

2. Model setup

According to the theory of dislocations [19], the plastic deformation of a metal is mediated by dislocation glide. As shown in Fig. 1(a), consider a crystal of unit volume containing some mobile dislocations, under a sufficiently high applied shear stress along the direction of Burgers vector b, dislocations glide causes a relative shift distance L of the material. If a dislocation moves completely across the slip plane with the width of crystal d, it contributes b to the total displacement L (Fig. 1(b)). Since b is small in comparison to d and the height of crystal h, the contribution made by a dislocation which moves a distance x_i may be taken as the fraction (x_i/d) of b. Thus, if the total number of mobile dislocations is N_t, the total displacement is,

$$L = \frac{b}{d}\sum_{i=1}^{N_t} x_i \tag{1}$$

and the macroscopic plastic shear strain ε is given by,

$$\varepsilon = \frac{L}{h} = \frac{b}{hd}\sum_{i=1}^{N_t} x_i \tag{2}$$

The ability of a metal to sustain plastic deformation is characterized by the number of mobile dislocations and their mean free path. If the metal could sustain a critical plastic shear strain (ε_c), it is ductile; otherwise, the metal is brittle. The mean free path $\bar{x}_i$ of mobile dislocations is a function of the grain size d and the dislocation density ρ_t=N_t for unit volume [20], thus:

$$\frac{1}{\bar{x}_i} = \frac{1}{d} + \frac{\sqrt{\rho_t}}{c} \tag{3}$$

where c is a hardening constant—a material–dependent parameter. In this work, we used $c = 10$ for calculation according to Ref. [20]. The dislocation mean free path is proportional to grain size, while inversely proportional to the dislocation density.

Once the mean free path of mobile dislocations is known, the number of mobile dislocations is the key to determine the plastic deformation of a metal. Here, we propose a theoretical formulation based on the relative ratio of the screw versus edge dislocation velocities as a factor for dislocation multiplication in BCC metals. The total number of mobile dislocation (ρ_t) including two parts, one part is the initial mobile dislocation density (ρ_i), and the other one is the mobile dislocations generated during plastic deformation via Frank-Read source (ρ_{F-R}), or emitted from grain boundaries (GB) (ρ_{GB}) or other likely sources. Thus the total number of mobile dislocation can be expressed as,

$$\rho_t = \rho_i + \alpha * (\rho_{F-R} + \rho_{GB} + n * \rho_{other}) \tag{4}$$

where $\alpha = v_s/v_e$ is the efficiency of dislocation sources, which determines the production rate of mobile dislocation via these sources. The symbol n gives the number of other types of dislocation sources. The generated dislocations from GB is written as: $\rho_{GB} = 3N_g/d$, where N_g (N_g=1.0 × 10^{10} m/m^2) is the dislocation length emitted from a unit area of metastable GB. The efficiency of dislocation source is controlled by $\alpha = v_s/v_e$ because their coordinative gliding governs dislocation multiplications [10,11]. Therefore, the number of initial mobile dislocations and the ability of dislocation multiplications determine the total number of mobile dislocation (ρ_t) in metals, thus controlling the deformability. If the temperature-dependent mobility of screw and edge dislocations is known, the efficiency of dislocation sources can be determined.

The mobility of dislocation can be estimated using the following equation [19],

$$V = \frac{\tau b}{B(T)} \tag{5}$$

where τ is the resolved shear stress and $B(T)$ is the drag (or friction) coefficient. $B(T)$ is dominated by the scattering of lattice vibrations (phonons), which is proportional to the temperature. Dislocation mobility depends on applied shear stress, purity of crystal, temperature and type of dislocations. In the low temperature and low-stress regimes, dislocation mobility is governed by kink-pair nucleation and migration [21–23], with the Gibbs free energy for kink-pair formation, ΔG_{kp}, written as $\Delta G_{kp} = \Delta H_{kp} - T\Delta S_{kp}$. Here ΔH_{kp} is the formation enthalpy, and ΔS_{kp} is the formation entropy. The enthalpy term is usually written as $\Delta H_{kp} = \Delta H_0\{[1 - (\frac{\tau}{\tau_p})^p]^q\}$, where ΔH_0 is a pre-factor related to the kink-pair formation energy, p and q are fitting parameters, τ

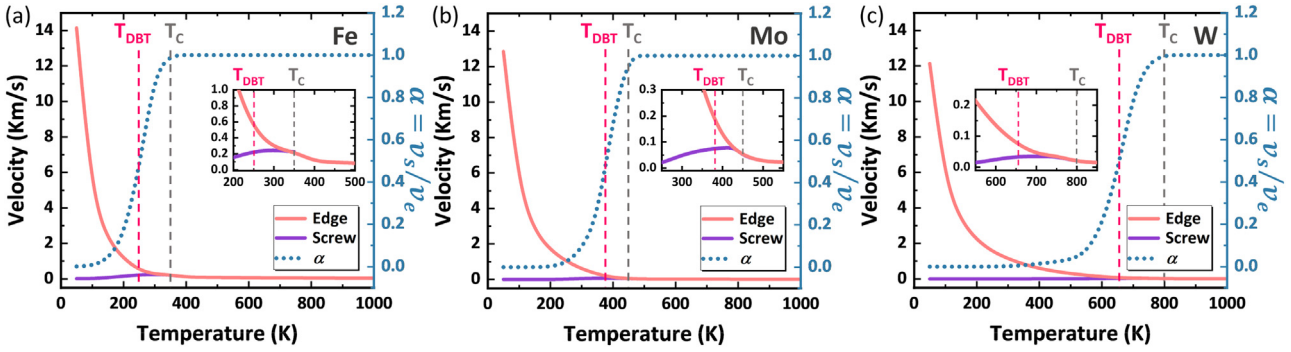

Fig. 2. The variation of dislocation velocity and the relative mobility of screw vs. edge as a function of temperatures in pure (a) Fe, (b) Mo, (c) W. DBTT is determined according to $\alpha = v_s/v_e = 0.5$. T_C is the critical temperature at which screw and edge dislocations have similar mobility. The insets highlight the variation of dislocation velocity around T_{DBT} and T_C.

Table 1
List of parameters used to estimate the dislocation mobility and DBTT in Fe, Mo and W [21–31]. The DBTT obtained from experiments are also involved for comparision.

	ΔH_0 (eV)	τ_p (MPa)	T_c (K)	B_e (Pa s/K)	B_k (Pa s)	p	q	DBTT (K)(Mod.)	DBTT (K) (Exp.)
Fe	0.84	363	350	8.8×10^{-8}	2.4×10^{-4}	0.54	1.04	250	198–230
Mo	1.27	840	450	2.6×10^{-7}	4.5×10^{-5}	0.995	1.02	380	348–383
W	1.63	960	800	3.3×10^{-7}	8.3×10^{-5}	0.999	1	657	600–773

is the applied shear stress and τ_p is the Peierls stress. The entropy term ΔS_{kp} is simplified and approximated as a constant term by, $\Delta S_{kp} = \Delta H_0 / T_C$, where T_C is the critical temperature of materials [12,21]. Thus, the free energy of kink-pair formation becomes: $\Delta G_{kp}(\tau, T) = \Delta H_0\{[1-(\frac{\tau}{\tau_p})^p]^q - \frac{T}{T_c}\}$. Following the dislocation mobility law of BCC metals developed in Ref. [21], if the $\Delta G_{kp}(\tau, T) > 0$, the velocity of screw dislocation can be expressed as,

$$V_s = \frac{\tau b}{B_k} \exp\left(-\frac{\Delta G_{kp}(\tau, T)}{2k_B T}\right) \quad (6)$$

where B_k is the drag coefficient related to the kink-pair mechanism. As the stress and temperature increases to the critical value, the dislocation motion will transfer into a phonon-drag regime ($\Delta G_{kp}(\tau, T) \le 0$), which shows a linear relationship with the applied stress. In accordance with the phonon-scattering theory [21], the velocity of edge dislocation can be written as,

$$V_e = \frac{\tau b}{B_e T} \quad (7)$$

The relative mobility, $\alpha = v_s/v_e$, is an indicator of the effectiveness of the dislocation sources operating in the BCC lattice [10]. A sufficiently high dislocation source efficiency is a prerequisite for initiating adequate plasticity in the crystal to avoid brittleness.

3. Results

Using the above model, we calculated the mobility of dislocations and the relative mobility of screw versus edge dislocations in pure iron (Fe), molybdenum (Mo), and tungsten (W), as shown in Fig. 2. Table 1 summaries the parameters used in the dislocation mobility calculations [21–31]. The critical temperature (T_C) is defined as the transition from a thermal to an athermal regime, at or above which the edge and screw dislocations have similar mobility [21–24]. In this work, the T_C of BCC metals are determined according to the experimental data [24–26]. Here, we follow the boundary condition: once the temperature reaches the T_C, the screw dislocation velocity equals to the edge dislocation velocity ($\Delta G_{kp}(\tau, T) \le 0$). Below T_C, the edge dislocation has higher mobility than that of the screw dislocation. Different from the kink-pair mechanism of screw dislocations, the glide of edge dislocations is governed by phonon drag, which is proportional to the temperature [21–23]. Therefore, the edge dislocation velocity decreases rapidly with the increasing temperature, while screw dislocation velocity gradually increases with the assistance of thermal activation (Fig. 2). The different trends of edge and screw dislocation mobility induce a variation of $\alpha = v_s/v_e$ with temperature. As shown by the blue lines in Fig. 2, the relative mobility of screw versus edge dislocation displays an abrupt increase within a narrow temperature range. This is indicative of a sharp transition in the efficiency of the dislocation sources. Besides, the ½<111> {112} edge dislocation in iron shows kink-mediated mobility in a specific low-stress region, indicating a trend of increasing dislocation velocity with rising temperatures [32]. However, this model only considers phonon-mediated edge dislocations, and the effect of slip planes are not involved [21–23].

For a well-annealed, coarse-grained high-purity polycrystalline BCC metal, the initial dislocation density is about $\rho_i = 1.0 \times 10^{12}/m^2$ [19,33]. The multiplication of dislocations in this case is mainly through Frank-Read sources [19]. For simplicity, we assume the maximum number of dislocations generated via Frank-Read sources is $\rho_{F-R}=1.0 \times 10^{15}/m^2$, which is comparable to the saturated dislocation density in a heavily-deformed tough metal [19,34]. As proposed earlier [10], if $\alpha \ge 0.5$, the Frank-Read source operates efficiently; otherwise, dislocations have a hard time getting multiplied and the metal is brittle. The larger the α value, the tougher the materials. Here, we take the temperature at which $\alpha = 0.5$ as the DBTT, which corresponds to a critical number density of mobile dislocations for ductile deformation ($\rho_{ductile}=6.51 \times 10^{14}/m^2$).

Fig. 3(a, b) plot the total number of mobile dislocations and the shear plastic strain as a function of temperature. The total number of mobile dislocations is limited at low temperatures, and dislocation multiplication takes off in a narrow temperature range, as marked in Fig. 3(a), which indicates the abrupt change in the deformation ability of metals. Similarly, the shear plastic strain also displays a transition once the temperature reaches a threshold value for Fe, Mo and W. According to the $\alpha = 0.5$ criterion for coarse-grained BCC metals, the critical shear plastic strain for ductile deformation is about $\varepsilon_c \approx 0.0633-0.0696$ (corresponding to

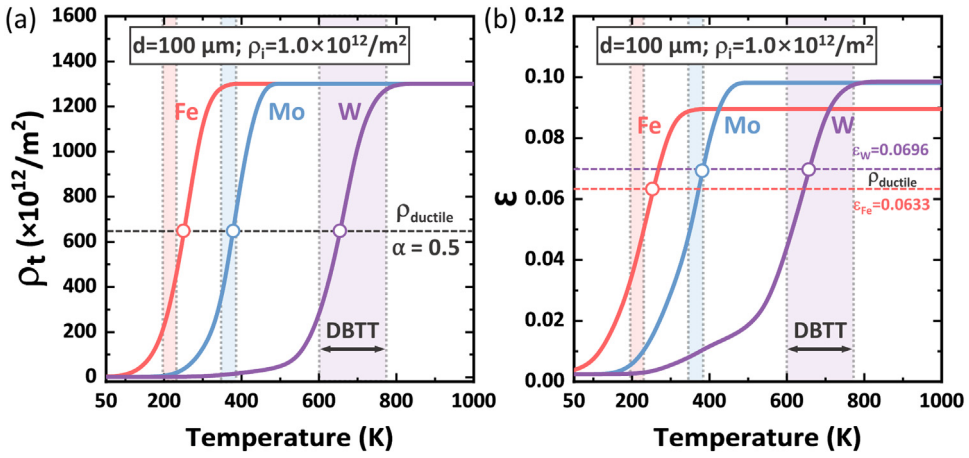

Fig. 3. Evolution of dislocation density and plastic shear strain with temperature. (a) Dislocation density vs. temperature in Fe, Mo and W. (b) Plastic shear strain vs. temperature in Fe, Mo and W. The dashed lines mark the critical mobile dislocation density and shear strain for DBT. The circles represent theoretically predicted DBTT, and the shaded areas show the experimental range of DBTT [12,30,31].

$\rho_{ductile}$) for Fe, Mo and W, as shown in Fig. 3(b). Since the critical strain is small, the dislocation dynamic recovery usually occurring at a larger plastic strain [35] is not considered in the model.

Actually, the variation in dislocation source efficiency determines the total number of mobile dislocation and the magnitude of shear plastic strain. In the low temperature range, the incompatibility between the fast-moving edge dislocations and the hard-moving screw dislocations limits dislocation multiplications [10,11]. As the mobile dislocations are unable to provide high enough shear plastic strain, the metal shows brittleness below DBTT. Once α reaches the critical value ($\alpha \geq 0.5$), the efficient operation of dislocation sources generates considerable number of mobile dislocations. As a result, the metal could carry more plastic shear strain, thus shows elevated toughness. The predicted DBTTs of Fe, Mo, and W are comparable with the experimental data, as shown in Fig. 3 and Table 1. It is the difference in dislocation behavior of Fe, Mo, and W that leads to the different DBTT [8].

4. Discussion

The toughness and brittleness of BCC metals are their intrinsic properties, governed by the dislocation activities, especially the relative mobility of screw versus edge dislocations. The glide of screw dislocations is sluggish below DBTT, however, with the edge dislocation having higher mobility at lower temperature range (Fig. 2). This give us a chance to tune the low temperature deformation ability of BCC metals.

According to experimental observations, the DBTT is strongly affected by some microstructural factors, such as grain size, initial dislocation density and alloying elements [11–16]. Hence, the effects of those additional factors on the DBT behavior are also explored. Fig. 4 shows the influence of grain size on the DBT behavior of Fe. Fig. 4(a) displays a shift of the dislocation density-temperature curves to the lower temperature range as the grain size decreasing from 100 μm to 1 μm for Fe with $\rho_i = 1.0 \times 10^{12}/m^2$. In this case, the generated dislocations from GBs become significant since the fraction of GB increases sharply at small grain sizes. The GB-emitted dislocations induce lower DBTT and better deformability, which is consistent with the reduced DBTT in ultrafine-grained BCC metals [14]. Furthermore, smaller grain size induced higher flow stress, promoting the nucleation of kink-pairs, thus higher mobility of dislocations and their relative mobility, corresponding to lower DBTT [36]. With further reducing the grain size down to nanometers, the restricted dislocations combined with the GB-mediated deformation may induce plastic instability in metals [37–39], corresponding to lowered toughness and tensile ductility [40,41]. Therefore, the nanocrystalline BCC metals are usually brittle because of the limited mean free path of dislocations in the nanometer-sized grains [40–43]. Fig. 4(b) compares the computations with the experimental data of commercial Fe and ferritic steel [41,44]. In general, the model can predict reasonably well the trend of experimental observations.

Fig. 5(a) plots the variation of dislocation density as a function of ρ_i and temperature in W. According to the critical dislocation density criteria ($\rho_{ductile}=6.51 \times 10^{14}/m^2$), the DBTT for each case can be determined, as marked by the horizontal dash line in Fig. 5(a). Here, with increasing ρ_i, the DBTT shifts to the lower temperature range. This is in line with previous studies that pre-deformation shifts the DBTT of metals to lower temperature [11–13]. Therefore, the pre-existing dislocations are of great significance to toughening normally brittle BCC metals [11–15].

According to Eq. (4), in addition to the ρ_i, the number of various types of dislocation source (n) also affects the dislocation multiplication. Since Frank-Read source and GB are not the only dislocation sources in polycrystalline materials, especially in pre-deformed metals, the effect of other possible dislocation sources should also be involved. Fig. 5(b) shows the influence of n on the dislocation multiplication behaviors and DBTT. For simplicity, we assume that the other dislocation sources have the comparable dislocation generation ability as the Frank-Read sources when fully operated. Therefore, the maximum number of dislocations generated via other sources is set as $\rho_{other}=1.0 \times 10^{15}/m^2$. The DBTT also shifts toward the low temperature range when more dislocation sources are operative. This trend explains the BCC metals with a laminated structure or second phase particles are tougher because interfaces serve as internal dislocation sources [45–47]. Fig. 5(c) displays the synergy effects of ρ_i, d and n on the DBTT of W. With the increasing of both ρ_i and n, the DBTT of W could be markedly decreased. For coarse-grained W ($n = 0$), enhancing both ρ_i and n can effective reduce the DBTT, as shown in Fig. 5(c). The decrease rate of DBTT is faster for $n < 2$ and then transits into a slow stage with further increasing of n. This is likely because of more dislocation source variants may further decrease the mean free path of dislocations. However, the effect of n becomes inconsequential for the sample with grain size of 1 μm, because in this case the GB-emitted dislocations control the plasticity. When all these tuning parameters are adopted, including ρ_i, n and d, the DBTT of W can be reduced down to below 0 °C, which is comparable to the real experimental data of cold-rolled or warm-rolled W in Fig. 5(d) [12,13]. Our predictive model suggests that higher ρ_i

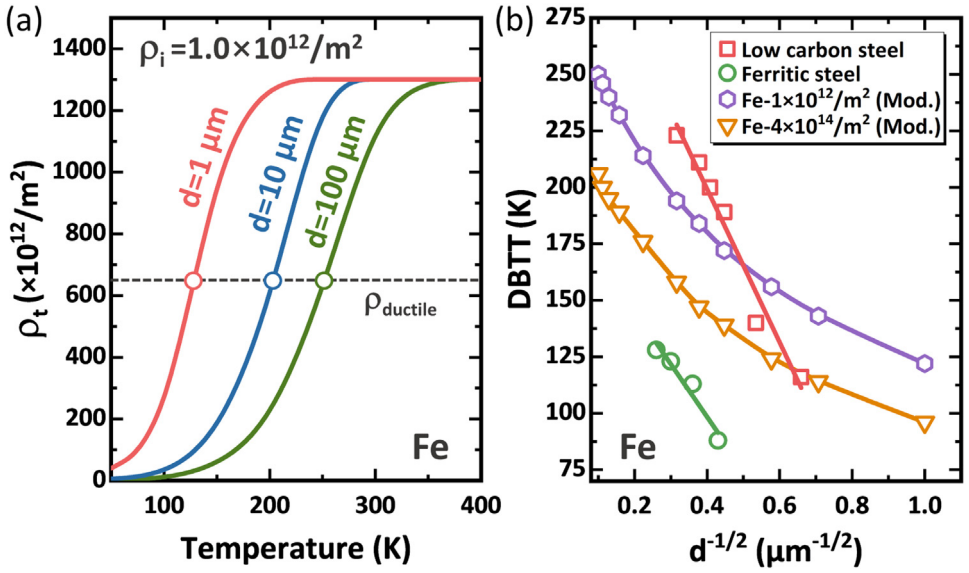

Fig. 4. Influence of grain size on the DBT behavior of Fe. (a) Evolution of dislocation density with grain sizes in Fe. The maximum total dislocation density is ρ_t =1.3 × 10^{15}/m^2. (b) Grain size-dependent DBTT in Fe and steel: modeling vs. experiment [41,44].

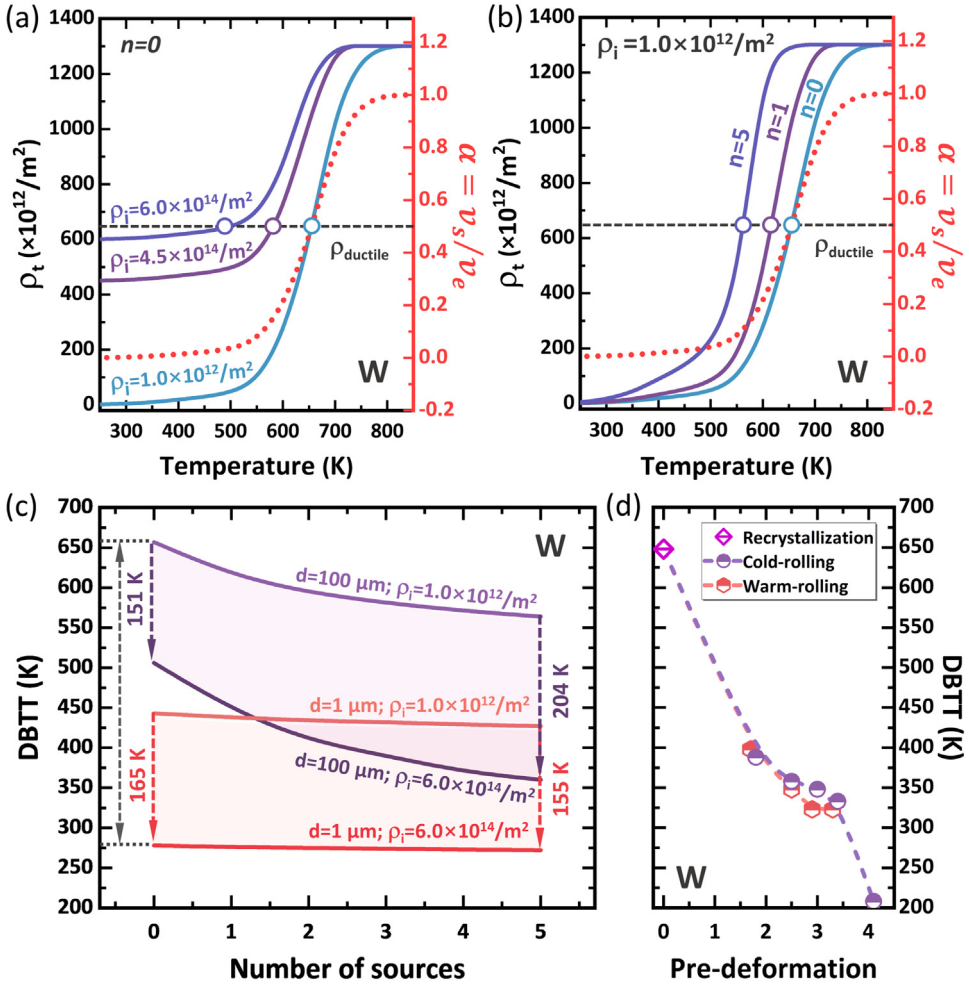

Fig. 5. Influence of grain size, initial dislocation density and variant of dislocation sources on the DBT behavior of W. Evolution of dislocation density with (a) initial dislocation density and (b) dislocation source species in W. The maximum total dislocation density is ρ_t =1.3 × 10^{15}/m^2. (c) Regulation of DBTT in W by tuning grain size, initial dislocation density and number of dislocation sources. (d) Decreasing of DBTT of W with different degree of pre-deformation in experiments [12,13].

combined with smaller grain size achieve the best toughening in the BCC metals [12–15]. Because not only numerous pre-stored dislocations, but the interfaces, precipitates or helium bubbles could operate as dislocation sources [45–50], which can all be used to tune the toughness of BCC metals.

5. Conclusion

In summary, we have formulated a quantitative model that can predict the DBT behavior, in particular the DBTT, of various BCC metals, based on the relative mobility of screw versus edge dislocations, which governs dislocation multiplications via Frank-Read sources. The new model is also extended to include other contributors that make mobile dislocations available, covering the influence of the initial dislocation density, grain size and the multitude of dislocation sources, offering a useful guide for the design of tougher BCC metals.

Declaration of Competing Interest

The authors declare that there is no conflict of interest.

Acknowledgments

This research was supported by the National Natural Science Foundation of China (Grant Nos. 51922082 and 51971170) and the “111 Project" of China 2.0 (Grant No. BP0618008). E.M. acknowledges XJTU for hosting his work at the Center for Alloy Innovation and Design.

References

[1] J.W. Christian, Metall. Trans. A 14 (1983) 1237–1256.
[2] S.G. Roberts, A.S. Booth, P.B. Hirsch, Mater. Sci. Eng. A 176 (1994) 91–98.
[3] C. St. John, Philos. Mag. 32 (1975) 1193–1212.
[4] E. Tarleton, S.G. Roberts, Philos. Mag. 89 (2009) 2759–2769.
[5] J.R. Rice, R. Thomson, Philos. Mag. 29 (1974) 73–97.
[6] P. Gumbsch, J. Riedle, A. Hartmaier, H.F. Fischmeister, Science 282 (1998) 1293–1295.
[7] V. Vitek, Philos. Mag. 84 (2004) 415–428.
[8] A. Seeger, Int. J. Mater. Res. 93 (2002) 760–777.
[9] D. Rodney, L. Ventelon, E. Clouet, L. Pizzagalli, F. Willaime, Acta Mater. 124 (2017) 633–659.
[10] Y. Lu, Y.H. Zhang, E. Ma, W.Z. Han, Proc. Natl. Acad. Sci. U. S. A. 118 (2021) e2110596118.
[11] Y.H. Zhang, W.Z. Han, Acta Mater. 220 (2021) 117332.
[12] C. Bonnekoh, J. Reiser, A. Hartmaier, S. Bonk, A. Hoffmann, M. Rieth, J. Mater. Sci. 55 (2020) 12314–12337.
[13] C. Bonnekoha, U. Jäntscha, J. Hoffmanna, H. Leistea, A. Hartmaierb, D. Weygandc, A. Hoffmannd, J. Reiser, Int. J. Refract. Met. Hard Mater. 78 (2019) 146–163.
[14] A.A.N. Németh, J. Reiser, D.E.J. Armstrong, M. Rieth, Int. J. Refract. Met. Hard Mater. 50 (2015) 9–15.
[15] X.F. Xie, Z.M. Xie, R. Liu, Q.F. Fang, C.S. Liu, W.Z. Han, X. Wu, Acta Mater. 228 (2022) 117765.
[16] Z.M. Xie, R. Liu, S. Miao, X.D. Yang, T. Zhang, X.P. Wang, Q.F. Fang, C.S. Liu, G.N. Luo, Y.Y. Lian, X. Liu, Sci. Rep. 5 (2015) 16014.
[17] P.B. Hirsch, S.G. Roberts, Philos. Mag. A 64 (1991) 55–80.
[18] M. Khantha, D.P. Pope, V. Vitek, Phys. Rev. Lett. 73 (1994) 684–687.
[19] D. Hull, D.J. Bacon, Introduction to Dislocations, 5th ed., Elsevier, Oxford, 2011.
[20] D. Cereceda, M. Diehl, F. Roters, P. Shanthraj, D. Raabe, J.M. Perlado, J. Marian, GAMM-Mitt. 38 (2015) 213–227.
[21] G. Po, Y. Cui, D. Rivera, D. Cereceda, T.D. Swinburne, J. Marian, N. Ghoniem, Acta Mater. 119 (2016) 123–135.
[22] B. Chen, S. Li, H. Zong, X. Ding, J. Sun, E. Ma, Proc. Natl. Acad. Sci. U. S. A. 117 (2020) 16199.
[23] Y. Cui, G. Po, N. Ghoniem, Acta Mater. 108 (2016) 128–137.
[24] E. Kuramoto, Y. Aono, K. Kitajima, Scr. Metall. 13 (1979) 1039–1042.
[25] R. Gröger, V. Vitek, Acta Mater. 56 (2008) 5426–5439.
[26] D. Brunner, Mater. Trans. JIM 41 (2000) 152–160.
[27] C.R. Weinberger, Acta Mater. 58 (2010) 6535–6541.
[28] F. Maresca, D. Dragoni, G. Csányi, N. Marzari, W.A. Curtin, npj Comput. Mater. 4 (2018) 69.
[29] J. Chang, W. Cai, V.V. Bulatov, S. Yip, Comput. Mater. Sci. 23 (2002) 111–115.
[30] C. Minnert, H. ur Rehman, K. Durst, J. Mater. Res. 36 (2021) 2397–2407.
[31] W.A. Spitzig, Metall. Trans. 3 (1972) 1183–1188.
[32] S. Queyreau, J. Marian, M.R. Gilbert, B.D. Wirth, Phys. Rev. B 84 (2011) 064106.
[33] S. Naamane, G. Monnet, B. Devincre, Int. J. Plast. 26 (2010) 84–92.
[34] B.B. He, B. Hu, H.W. Yen, G.J. Cheng, Z.K. Wang, H.W. Luo, M.X. Huang, Science 357 (2017) 1029–1032.
[35] T.B. Yu, N. Hansena, X.X. Huang, A. Godfrey, Mater. Res. Lett. 2 (2014) 160–165.
[36] Q. Wei, J. Mater. Sci. 42 (2007) 1709–1727.
[37] S. Cheng, A.D. Stoica, X.L. Wang, Y. Ren, J. Almer, J.A. Horton, C.T. Liu, B. Clausen, D.W. Brown, P.K. Liaw, L. Zuo, Phys. Rev. Lett. 103 (2009) 035502.
[38] Q. Wei, S. Cheng, K.T. Ramesh, E. Ma, Mater. Sci. Eng. A 381 (2004) 71–79.
[39] Lihua Wang, Yin Zhang, Zhi Zeng, Hao Zhou, Jian He, Pan Liu, Mingwei Chen, Jian Han, David J. Srolovitz, Jiao Teng, Yizhong Guo, Guo Yang, Deli Kong, En Ma, Yongli Hu, Baocai Yin, XiaoXu Huang, Ze Zhang, Ting Zhu, Xiaodong Han, Science 375 (2022) 1261–1265.
[40] R. Song, D. Ponge, D. Raabe, Acta Mater. 53 (2005) 4881–4892.
[41] S. Takaki, K. Kawasaki, Y. Kimura, J. Mater. Process. Technol. 117 (2001) 359–363.
[42] D. Farkas, B. Hyde, Nano Lett. 5 (2005) 2403–2407.
[43] K.J. Hemker, Science 304 (2004) 221–223.
[44] N. Tsuji, S. Okuno, Y. Koizumi, Y. Minamino, Mater. Trans. 7 (2004) 2272–2281.
[45] G. Liu, G.J. Zhang, F. Jiang, X.D. Ding, Y.J. Sun, J. Sun, E. Ma, Nat. Mater. 12 (2013) 344–350.
[46] M.S. Ding, J.P. Du, L. Wan, S. Ogata, L. Tian, E. Ma, W.Z. Han, J. Li, Z.W. Shan, Nano Lett. 16 (2016) 4118–4124.
[47] J.W. Zhang, I.J. Beyerlein, W.Z. Han, Phys. Rev. Lett. 122 (2019) 255501.
[48] L.L. Li, Y.Q. Su, I.J. Beyerlein, W.Z. Han, Sci. Adv. 6 (2020) eabb6658.
[49] R.Y. Zheng, W.R. Jian, I.J. Beyerlein, W.Z. Han, Nano Lett. 21 (2021) 5798–5804.
[50] J.T. Li, I.J. Beyerlein, W.Z. Han, Acta Mater. 226 (2022) 117656.